

**Electron-spectroscopic investigation of metal-insulator transition  
in  $\text{Sr}_2\text{Ru}_{1-x}\text{Ti}_x\text{O}_4$  ( $x=0.0-0.6$ )**

Sugata Ray<sup>†</sup> and D. D. Sarma<sup>\*</sup>

*Solid State and Structural Chemistry Unit,  
Indian Institute of Science,  
Bangalore 560 012, INDIA*

R. Vijayaraghavan

*School of Science and Humanities,  
Vellore Institute of Technology Vellore 632 014, INDIA*

**Abstract**

We investigate the nature and origin of the metal-insulator transition in  $\text{Sr}_2\text{Ru}_{1-x}\text{Ti}_x\text{O}_4$  as a function of increasing Ti content ( $x$ ). Employing detailed core, valence, and conduction band studies with x-ray and ultraviolet photoelectron spectroscopies along with Bremsstrahlung isochromat spectroscopy, it is shown that a hard gap opens up for Ti content  $\geq 0.2$ , while compositions with  $x < 0.2$  exhibit finite intensity at the Fermi energy. This establishes that the metal-insulator transition in this homovalent substituted series of compounds is driven by Coulomb interaction leading to the formation of a Mott gap, in contrast to transitions driven by disorder effects or band filling.

PACS number(s): 71.30.+h, 79.60.-i, 71.20.-b, 71.28.+d

## I. INTRODUCTION

Oxide systems possessing  $K_2NiF_4$  and related structures have been extensively studied owing to their interesting structural, magnetic, and electrical properties. Recently, it was discovered that  $Sr_2RuO_4$ , a noncuprate member of  $A_2BO_4$  family, exhibits<sup>1</sup> superconductivity at 0.93 K. This report has naturally provoked many researchers to study the similarity and the dissimilarity between the superconductivity in this compound and that in the well-known  $La_2CuO_4$  with the same crystal structure, but a much higher  $T_c$  [Ref. 2]. The technique of substituting Cu by impurity ions in  $La_2CuO_4$  has been successfully used as a powerful probe to reveal the unconventional properties of this cuprate.<sup>3</sup> Similarly, various attempts have been made with  $Sr_2RuO_4$  by replacing Ru by Ir [Ref. 4], Fe [Ref. 5] and Ti [Ref. 6] ions, in order to investigate the effect of cationic substitutions. Nonmagnetic impurities are known to induce local moments and suppress  $T_c$  severely<sup>7</sup> and therefore, replacement of  $Ru^{4+}$  ( $4d^4$ ) ions by nonmagnetic  $Ti^{4+}$  ( $3d^0$ ) ions is an interesting topic of study. The synthesis of these doped ruthenates is relatively easy, since the  $Ti^{4+}$  ion has the same oxidation state, coordination number as well as very similar ionic radius when compared with  $Ru^{4+}$ . In fact, the compound  $Sr_2TiO_4$  is iso-structural with  $Sr_2RuO_4$  with very similar lattice parameters, making the substitution facile. It has been reported<sup>8</sup> that the  $Ti^{4+}$  impurity indeed suppresses the superconductivity and induces localized moments even for very low Ti concentration,  $x < 0.03$  in  $Sr_2Ru_{1-x}Ti_xO_4$ . During the past few years, a few reports have appeared<sup>9,10,11</sup> investigating Ti doped  $Sr_2RuO_4$  system; all these studies focus on the limit of very low Ti doping. Interestingly,  $Sr_2Ru_{1-x}Ti_xO_4$  is also expected to show a metal to insulator transition as a function of Ti doping, because the two end members possess widely different electrical properties with  $Sr_2RuO_4$  being a paramagnetic metal and  $Sr_2TiO_4$  being a band insulator. However, there are only few reports on the full series ( $0 \leq x \leq 1$ , in  $Sr_2Ru_{1-x}Ti_xO_4$ ) of compounds<sup>6,12</sup> investigating the transport properties, while no detailed electronic structure study has been reported to date. These transport studies reveal that there is a strong anisotropy between the interlayer resistivity ( $\rho_c$ ) and in-plane resistivity ( $\rho_{ab}$ ), observed in single crystal  $Sr_2RuO_4$ .<sup>8,9</sup>  $\rho_c$  of  $Sr_2RuO_4$  shows pure metallic conductivity below 130 K and nonmetallic  $d\rho_c / dT < 0$  at higher temperatures. However, the metal-nonmetal crossover temperature decreases with increasing  $x$  (Ti concentration) and for  $x=0.2$ ,  $\rho_c$  never enters a metallic regime. The in-plane resistivity remains metal-

lic throughout the temperature range for  $\text{Sr}_2\text{RuO}_4$ , while with increasing  $x$ , an insulating upturn is observed in the resistivity data. For  $x=0.2$  sample, such semiconducting-like behavior is found below 40 K [Ref. 9]. Moreover, Oswald *et al.*<sup>6</sup> reported a steep increase in the room temperature resistivity of polycrystalline  $\text{Sr}_2\text{Ru}_{1-x}\text{Ti}_x\text{O}_4$  compounds at around  $x = 0.3$ . Therefore, all these observations indicate the occurrence of a metal to insulator transition (MIT) as a function of Ti doping in this ruthenate series, the critical composition being close to  $x=0.2$ .

In order to understand the electronic structure and thereby the nature of the MIT in this series, we have carried out a detailed high-energy spectroscopic study on  $\text{Sr}_2\text{Ru}_{1-x}\text{Ti}_x\text{O}_4$  for  $x=0.0, 0.1, 0.2, 0.5$  and  $0.6$ , employing x-ray photoelectron (XP), ultraviolet photoelectron (UP), and Bremsstrahlung isochromat (BI) spectroscopies (S). These experimental studies, supplemented by band structure calculations for  $\text{Sr}_2\text{RuO}_4$  and  $\text{Sr}_2\text{TiO}_4$ , using an *ab initio* self-consistent linearized-muffin-tin orbital (LMTO) method within the atomic sphere approximation (ASA), establish the importance of Coulomb correlation effects in understanding metal insulator transition as a function of Ti concentration, which can only be analyzed in terms of Mott transition.

## II. EXPERIMENTAL AND THEORETICAL DETAILS

All electron spectroscopic studies reported here were carried out on polycrystalline samples which were synthesized by the conventional ceramic route. Stoichiometric quantities of high purity  $\text{SrCO}_3$  and the respective transitional metal oxides were thoroughly ground and the mixture was heated at 600 °C for 24 h to avoid Ru evaporation, then at 930 °C for 24 h, then at 1050 °C for 24 h, and finally at 1200 °C for 36 h with intermittent grindings. The product was then pressed into pellets and finally sintered at 1200 °C for 36 hours and cooled to room temperature in air. The phase purity of each composition was checked by powder x-ray diffraction (XRD) technique. A transport study of these compounds has already been published.<sup>12</sup>

Electron spectroscopic studies were carried out in a commercial spectrometer from VSW Scientific Instruments Ltd., United Kingdom, equipped with a monochromatized Al  $K\alpha$  photon source for XPS, a He discharge lamp for UPS, and an electron gun for BIS. The samples were mounted on copper stubs using ultrahigh vacuum (UHV) compatible resins,

while the electrical contact of the sample with the instrument ground was maintained using UHV compatible Ag paste. The pressure of the experimental chamber was better than  $5 \times 10^{-10}$  mbar during the experiment and the sample surface was cleaned *in situ* by mechanical scraping using an alumina file until the various core levels (O 1s and Sr 3d) showed reproducible spectral features and also the intensity of adventitious C 1s peak was reduced to a minimum. All experiments were performed at room temperature. The binding energy of all spectral features were calibrated to the instrument Fermi level which was determined by recording the Fermi edge region from a clean silver sample.

Self-consistent LMTO-ASA calculations were performed for stoichiometric  $\text{Sr}_2\text{RuO}_4$  and  $\text{Sr}_2\text{TiO}_4$  in the experimentally determined tetragonal structure with seven atoms per unit cell and with 128  $k$  points in the irreducible part of the Brillouin zone. The lattice parameters used for  $\text{Sr}_2\text{RuO}_4$  are  $a=b=3.8603 \text{ \AA}$  and  $c=12.729 \text{ \AA}$  (Ref. 13) and for  $\text{Sr}_2\text{TiO}_4$  are  $a=b=3.88 \text{ \AA}$  and  $c=12.6 \text{ \AA}$  (Ref. 14).

### III. RESULTS AND DISCUSSION

In Fig. 1(a), we show the spectral region for Ru 3p and Ti 2p core levels for these compounds. For  $\text{Sr}_2\text{RuO}_4$  (*i.e.*,  $x=0$  sample), we observe a doublet feature with peaks at 463.8 eV for Ru  $3p_{3/2}$  and 486.4 eV for Ru  $3p_{1/2}$  core level spectra with a spin-orbit splitting of 22.6 eV. Weak satellite features are also seen at around 476.5 and 499 eV, corresponding to main Ru  $3p_{3/2}$  and  $3p_{1/2}$  features, respectively. A new distinct peak appears next to the Ru  $3p_{3/2}$  peak at 458 eV, gaining intensity monotonically with increasing Ti doping in  $\text{Sr}_2\text{Ru}_{1-x}\text{Ti}_x\text{O}_4$ ; this is identified as the Ti  $2p_{3/2}$  signal. The spin-orbit splitting in 2p level of  $\text{TiO}_2$  [Ref.15] is around 5.7 eV, therefore, Ti  $2p_{1/2}$  signal appears at around 463.7 eV binding energy, overlapping the Ru  $3p_{3/2}$  signal. In order to investigate the Ti 2p core level spectral features without the overlapping Ru 3p core level signal, we used the Ru 3p signal from the  $\text{Sr}_2\text{RuO}_4$  ( $x=0$ ) sample as the reference spectrum for Ru 3p spectral shape for all the compounds. The basic idea is to remove the Ru 3p contribution from the spectral region in Fig. 1(a) by subtracting the reference Ru 3p spectrum, obtained from the parent undoped  $\text{Sr}_2\text{RuO}_4$ , after a proper multiplicative normalization; thus extracted Ti 2p spectra are shown for all  $x>0$  in Fig. 1(b). Resulting Ti  $2p_{3/2}$  and  $2p_{1/2}$  peaks appear at 458 and 463.7 eV binding energies, with the expected spin-orbit splitting of 5.7 eV for a  $\text{Ti}^{4+}$

species. Moreover it is well known that  $\text{Ti}^{4+}$  oxides, as in  $\text{SrTiO}_3$  [Ref. 16] or  $\text{TiO}_2$  [Refs. 15, 16], show weak satellite features, at about 13 eV away from the main peak in the Ti  $2p$  spectral region, characteristic of the  $\text{Ti}^{4+}$  state. In the present case, we can see similar weak satellite features at about 13 eV above the main peaks in the extracted Ti  $2p$  spectra, [marked by arrows in Fig. 1(b)]. This confirms that Ti is in the formally  $\text{Ti}^{4+} 3d^0$  state in this family of compounds, establishing this as a homovalent substituted ( $\text{Ti}^{4+}$  in place of  $\text{Ru}^{4+}$ ) family of compounds. It is important to note here that such homovalent substitutions leave the electronic configuration of Ru sites essentially unchanged, in contrast to more usual heterovalent substitutions (e.g.,  $\text{Sr}^{2+}$  in place of  $\text{La}^{3+}$ ) leading to a doping of charge carriers into the system.

In Fig. 2, we show the calculated density of states (DOS) of the two end members, namely,  $\text{Sr}_2\text{RuO}_4$  and  $\text{Sr}_2\text{TiO}_4$ . In the upper panel [Fig. 2(a)], we show the total DOS along with the Ru  $d$ , O  $p$ , Sr  $d$ , and Sr  $s$  partial DOS for  $\text{Sr}_2\text{RuO}_4$ . The total DOS has a finite value at  $E_F$ , consistent with the metallic property of  $\text{Sr}_2\text{RuO}_4$ . The occupied part of the DOS is dominated by O  $p$  and Ru  $d$  states. Significant amounts of O  $p$  states extend down to about -7.8 eV with three distinct groups of features, namely, those between -3.5 and -7.8 eV, between -1.7 and -3 eV and very close to the Fermi energy. The Ru  $d$  states are found to spread over the complete valence band range down to -7.8 eV. The feature near -6 eV is contributed by the bonding O  $p$  states with Ru  $d$  states. The most intense feature around -2.5 eV in the total DOS corresponds to primarily O  $2p$  states nonbonding with respect to Ru-O interactions and therefore, with a negligible contribution from Ru states. Ru ions in  $\text{Sr}_2\text{RuO}_4$  remains in the low-spin configuration ( $4d^4 : t_{2g}^4$ ) because of a strong crystal field effect<sup>17</sup> splitting the  $e_g$  and the  $t_{2g}$  levels significantly. Therefore, it has been shown that the states at  $E_F$  arises from the antibonding Ru  $d\epsilon(xy, yz, zx)$  and O  $p\pi$  states having four electron occupancy in these triply degenerate bands.<sup>13,18</sup> The unoccupied DOS between 0 and 3.5 eV is dominated by Ru  $d e_g$ -derived states, while the states around 7 eV is contributed mainly by Sr  $d$  related states. All the features above 10 eV in the unoccupied DOS are mainly contributed by Sr  $s$  and  $p$  states along with O  $s$  states.

The calculated band structure for  $\text{Sr}_2\text{TiO}_4$  is shown in Fig. 2(b). It exhibits a clear gap between the occupied and the unoccupied states, in agreement with the observed insulating property of the compound, in contrast to the metallic state of  $\text{Sr}_2\text{RuO}_4$ . The Fermi level in Fig. 2(b) has been aligned at the bottom of the conduction band. The calculation indicates

a band gap of 1.3 eV. Expectedly, the occupied part of the band is completely dominated by the O  $p$  states with small contributions from Sr  $d$  and Ti  $d$  states, consistent with the idea of a formal  $\text{Ti}^{4+}$  ( $d^0$ ) valence state in the compound. The Ti  $d$  level has some occupancy arising from the hybridization of Ti  $d$  states with the O  $p$  states. The feature centered at about -5 eV in the total DOS is found to have significant contributions from such hybridized Ti  $d$  states along with the dominant O  $p$  contributions. The features around -3 eV are primarily from an admixture of O  $p$  and Sr  $d$  states. The first part (0 to 2.7 eV) of the unoccupied density of states is completely dominated by Ti  $d$  states of  $t_{2g}$  symmetry, while the Ti  $e_g$  states appear between 2.5 and 7.5 eV, strongly admixed with a contribution from Sr  $d$  states. The features above 12 eV has contributions from Sr  $s$ , O  $s$ , and Ti  $p$  states.

The experimental XPS valence band spectra from all the samples are shown in Fig. 3. The overall spectral features of the valence band are similar for all the compounds, though there are some systematic variations in the relative intensities as well as in spectral details of different features. The XP spectra exhibit two broad features with peaks at about 1.5 and 5.7 eV binding energies, respectively. The broad feature centered near 5.7 eV binding energy is easily seen to be due to primarily O  $p$  bonding states for all compositions; this is evident from the fact that both  $\text{Sr}_2\text{RuO}_4$  and  $\text{Sr}_2\text{TiO}_4$  have O  $p$  DOS over this energy range (see Fig. 2). The spectral intensity of the 1.5 eV feature decreases monotonically with increasing Ti doping. An intensity decrease of certain parts over the occupied states is indeed to be expected in view of a progressive substitution of  $\text{Ru}^{4+} 4d^4$  state by  $\text{Ti}^{4+} 3d^0$  state with an increasing  $x$  in this series. A comparison with the band structure results of  $\text{Sr}_2\text{RuO}_4$  [see Fig. 2(a)] reveals that the spectral feature with the peak at 1.5 eV is mainly contributed by O  $p$  nonbonding states over the higher energy between 1.5 and 3.5 eV binding energy and the antibonding Ru  $d\epsilon$ -O  $p\pi$  states at a lower energy near the Fermi level. In the case of  $\text{Sr}_2\text{TiO}_4$ , on the other hand, a gap opens up near  $E_F$  over the energy window where Ru  $4d$  states are found in  $\text{Sr}_2\text{RuO}_4$ , due to the  $3d^0$  configuration of the  $\text{Ti}^{4+}$  in contrast to  $4d^4$  configuration of  $\text{Ru}^{4+}$ . The O  $p$  nonbonding contributions in  $\text{Sr}_2\text{TiO}_4$  appear around 1.5–2 eV binding energy as also in the case of  $\text{Sr}_2\text{RuO}_4$ . Therefore, with increasing Ti concentration, the Ru-O antibonding states close to Fermi energy are progressively removed, resulting in a decrease in the overall spectral intensity in the 0–2 eV binding energy region, as observed in the experimental spectra. While such considerations provide an understanding of the overall decrease in the spectral intensity within the first 2 eV of the Fermi energy with

increasing  $x$ , these fail to explain a more interesting, though subtle, aspect of the spectral change. First we note that the spectral intensity at  $E_F$  is substantial for  $\text{Sr}_2\text{RuO}_4$ , as is evident in Fig. 3, consistent with its metallic ground state. It is also evident from the figure that there is negligible intensity at  $E_F$  for  $x=0.6$ , also consistent with its insulating ground state, thereby capturing the change in the electronic structure associated with the experimentally observed metal-insulator transition. However, it is clear that the previous discussion indicating a decrease in the spectral intensity will invariably suggest a finite intensity at the  $E_F$ , proportional to the Ru content. In other words, the naive description of an overall decrease of the Ru  $4d$  associated spectral intensity and the associated changes in the electronic structure cannot explain the absence of any spectral intensity at  $E_F$  for any finite  $x$  less than 1 and therefore, such an approach cannot explain the metal-insulator transition at a fractional  $x$  value in this series. We note that the spectral behavior in the near  $E_F$  region suggests the formation of a gap even at a finite Ru concentration; such a gap formation is well known in the context of insulating transition metal compounds, driven by Coulomb interactions. However, a poor instrumental resolution in XPS precludes any careful investigation of the gap formation as a function of  $x$  in these spectra. This issue will be discussed in greater detail at a later stage, making use of the higher resolution in UP spectra. However, we note here that the correlation effect in this Ru  $4d$  band system has been shown<sup>18</sup> to be unexpectedly strong and cannot be ignored.

Changes in the electronic structure near the Fermi edge region are most directly responsible for the metal-insulator transition in any system and therefore, this spectral region is the most important one to understand the nature of the MIT in this series of compounds. We have carefully studied the narrow spectral region close to the Fermi energy for all the samples, using He I UPS, in view of its much better energy resolution. The set of He I narrow scan spectra, emphasizing the changes in the electronic structure close to the Fermi energy, is shown in Fig. 4. All the spectra are normalized at 2.8 eV binding energy, because this intensity is almost completely derived from O  $2p$  nonbonding states which remain invariant with Ti doping. We observe nearly the same intensity for all the spectra at about 2 eV binding energy; these spectral features are primarily contributed by nonbonding O  $p$  states (see Fig. 2) providing an explanation for the near constancy of this spectral feature across the series. The regular decrease in spectral intensity with increasing Ti concentration in the 0 to 2 eV energy region is evident from the figure; this is essentially due to the substitution of the



$\text{Ru}^{4+} d^4$  with  $\text{Ti}^{4+} d^0$  configuration with increasing  $x$ , decreasing the total electron count. But more interestingly, we observe a very substantial gap ( $\sim 0.1\text{--}0.2$  eV) opening at  $E_F$  for  $x \geq 0.2$  compounds, thereby clearly signalling the metal-insulator transition, consistent with reports<sup>6,12</sup> based on transport measurements.

We have also probed the evolution of the unoccupied states as a function of Ti doping using BI spectroscopy. The experimental BI spectra, shown in Fig. 5, exhibit three broad features with peaks at 1.8, 10, and 17 eV. The spectra clearly exhibit finite DOS at  $E_F$  for  $x=0$  and 0.1 compounds; interestingly, the spectral intensity at  $E_F$  vanishes for  $x \geq 0.2$ , thereby defining an energy gap and an insulating state, consistent with the valence band results, discussed above. The feature extending from  $E_F$  up to about 5 eV decreases in intensity systematically with increasing  $x$ . This can be understood by considering the cross section of different states. It is known<sup>19</sup> that the cross section of Ru  $4d$  states is almost 100 times that of Ti  $3d$  states at an excitation energy of 1486.6 eV, employed in the present study. Therefore, spectra in the 0–3 eV range are dominated by Ru  $4d$  states, with only minor contributions from Ti  $3d$  states; this immediately explains the experimental observation of decreasing intensity of the leading spectral feature with increasing Ti doping in place of Ru. In contrast to the clear and systematic change in the spectral feature close to  $E_F$ , the higher energy features remain almost identical with changing Ti concentration. This is not surprising, as the band structure results indeed show that the features above 6 eV are dominated by O and Sr states, which are essentially the same for both  $\text{Sr}_2\text{RuO}_4$  and  $\text{Sr}_2\text{TiO}_4$ .

While all these spectroscopic results, establishing a metal-insulator transition, are consistent with transport properties,<sup>6,12</sup> these spectroscopic results provide some critical inputs in understanding the possible mechanism responsible for this MIT, clearly making several other alternative mechanisms untenable. Though the mechanism of the MIT in this system has hardly been discussed in the literature so far, our results, for example, clearly suggest that the MIT in this system cannot be understood in terms of percolation or any other inhomogeneous model, with the assumption that the doping of Ti in place of Ru in  $\text{Sr}_2\text{RuO}_4$  does not result in homogeneously doped samples, but only some inhomogeneous physical mixtures of the end compositions, namely,  $\text{Sr}_2\text{RuO}_4$  and  $\text{Sr}_2\text{TiO}_4$ . According to such a description, increasing Ti concentration should gradually increase the concentration of  $\text{Sr}_2\text{TiO}_4$  at the cost of metallic  $\text{Sr}_2\text{RuO}_4$  and consequently, a gradual reduction in the intensity of

the spectral feature at  $E_F$  with increasing Ti doping, is expected. More importantly, the spectra for even the insulating range of compounds with  $x \geq 0.2$  are expected to exhibit finite spectral weight at  $E_F$ , contributed by the large metallic fraction present in the inhomogeneous system representing a mixture of metallic and insulating phases. Evidently, this is not observed experimentally where a finite and substantial gap is found to appear in the spectral weight near  $E_F$  with only 20% Ti doping. Specifically, the changes in the lattice parameters between the end members [for  $\text{Sr}_2\text{RuO}_4$   $a=b=3.8603 \text{ \AA}$  and  $c=12.729 \text{ \AA}$  (Ref. 13) and for  $\text{Sr}_2\text{TiO}_4$   $a=b=3.88 \text{ \AA}$  and  $c=12.6 \text{ \AA}$  (Ref. 14)] are not large enough to make any perceptible change in the various hopping strengths that contribute to the bandwidth. Therefore, the only significant change in the bandwidth will be due to the decrease in the average coordination number by 20% at the same level of doping. Since the bandwidth is linearly proportional to the coordination number within a tight binding model, we may expect a decrease of about 20% in the Ru  $4d$  bandwidth from this homovalent substitution.

Another possible mechanism for the MIT is the disorder driven Anderson transition arising from random replacement of Ru ions by Ti in the  $\text{Sr}_2\text{RuO}_4$  lattice. It is indeed true that the extent of disorder is expected to increase with increasing Ti concentration at least until the point of 50% doping. Such disorder driven metal-insulator transition is likely to be signalled by a finite spectral weight at  $E_F$ , since the Anderson-type transitions are characterized by finite, but localized, density of states at  $E_F$ . In presence of long range Coulomb interactions such a system may even open up a soft gap, namely, Coulomb gap.<sup>20</sup> Electron spectroscopic investigations have indeed revealed<sup>21</sup> a host of interesting spectroscopic features associated with disorder effects in substituted transition metal compounds. However, the experimental observation of a substantial hard gap in the present case is clearly not compatible with ideas concerning a disorder-driven MIT.

The electronic configuration of  $\text{Ru}^{4+}$  ( $4d^4$ ) ion in  $\text{Sr}_2\text{RuO}_4$  is low-spin. While a strong crystal field would split the  $d$  levels into  $t_{2g}$  and  $e_g$  states, the Jahn-Teller distortion in  $\text{Sr}_2\text{RuO}_4$  with an elongation of the  $\text{RuO}_6$  octahedra along the  $z$ -axis further splits the triply degenerate  $t_{2g}$  level, leading to a stabilization of the doubly degenerate  $d_{zx}$ ,  $d_{yz}$  bands with respect to the  $d_{xy}$  band. If this effect is very strong, the system could go into an insulating state with a fully filled doubly degenerate  $d_{zx}$ ,  $d_{yz}$  band. However the extent of distortion is not very severe in  $\text{Sr}_2\text{RuO}_4$  and the spread of the  $d_{xy}$  band is wide enough to overlap with the  $d_{yz,zx}$  band.<sup>17</sup> As a consequence, the system remains metallic in spite of the modest

Jahn-Teller distortion. Doping with Ti would certainly narrow the Ru bandwidth; however, this effect is not expected to be large enough to remove the overlap of the  $d_{xy}$  band with the  $d_{yz}$  and  $d_{zx}$  bands altogether for as little as 20% Ti doping.

It has been already reported<sup>18</sup> that the electron correlation effect is not negligible in  $\text{Sr}_2\text{RuO}_4$  in spite of the broad Ru  $4d$  band. Therefore, the physical properties of these compounds are controlled by the relative strengths of on-site Coulomb interaction energy  $U$  and the bandwidth  $W$ . In the limit of  $U$  being significantly less than  $W$ , the system is metallic, while a progressive reduction in  $W$  can drive a metal to insulator transition in a system with integral  $d$  occupancy. We believe that this system is another example of such a bandwidth controlled MIT, in contrast to any band-filling controlled physics in spite of its obvious composition-driven change. Our core level study has shown that Ti retains its stable 4+ oxidation state throughout the series; as a consequence, the Ru ions throughout the series has an integral filling with  $4d^4$  electronic configuration. Random replacement of Ru ions by Ti ions has two distinct effects on the electron motion. Effects of disorder in such a case will definitely be present; however, as discussed above, it cannot explain the MIT. The second, and more important, consequence of the substitution in the present context is to reduce the Ru-Ru coordination; this evidently leads to decrease in the Ru  $4d$  bandwidth. Such a progressive reduction in  $W$  with increasing Ti concentration may lead to the value of  $U/W$  to cross the critical value for the metal-insulator transition leading to the insulating state with a finite Mott-Hubbard gap at the Fermi energy. This description of the MIT appears to be the only one compatible with all the experimental observations presented here.

In conclusion, we have investigated the electronic structure of  $\text{Sr}_2\text{Ru}_{1-x}\text{Ti}_x\text{O}_4$  with  $x=0.0, 0.1, 0.2, 0.5,$  and  $0.6$  using x-ray and ultraviolet photoemission spectra and high-energy Bremsstrahlung isochromat spectra in conjunction with *ab initio* band structure results. Core level spectra establish that substituted Ti remains in the  $\text{Ti}^{4+}$  state throughout the series, ensuring a  $\text{Ru}^{4+} 4d^4$  with integral Ru  $4d$  occupancy per Ru site. Spectra from the occupied and unoccupied parts show the formation of a gap ( $\sim 200$  meV) at the Fermi energy for samples with Ti content,  $x \geq 0.2$ , establishing a metal-insulator transition. These available results can only be understood in terms of a bandwidth controlled metal-insulator transition as a function of the composition, arising from a decreasing Ru-Ru coordination with increasing Ti content.

#### IV. ACKNOWLEDGEMENTS

The authors acknowledge the Department of Science and Technology, and the Board of Research in Nuclear Sciences, Government of India, for financial support.

- 
- <sup>†</sup> Present address: Materials and Structures Laboratory, Tokyo Institute of Technology, 4259 Nagatsuta, Midori-ku, Yokohama 226-8503, Japan.
- \* Also at Jawaharlal Nehru Centre for Advanced Scientific Research, Bangalore, and Center for Condensed Matter Theory, Indian Institute of Science, Bangalore, India. Electronic address: sarma@sscu.iisc.ernet.in
- <sup>1</sup> Y. Maeno, H. Hashimoto, K. Yoshida, S. Nishizaki, T. Fujita, J. G. Bednorz, and F. Lichtenberg, *Nature* **372**, 532 (1994).
- <sup>2</sup> J. G. Bednorz and K. A. Muller, *Z. Phys. B: Condens. Matter* **64**, 189 (1986).
- <sup>3</sup> Y. Maeno, T. Tomita, M. Kyogoku, S. Awaji, Y. Aoki, K. Hoshino, A. Minami, and T. Fujita, *Nature* **328**, 512 (1987).
- <sup>4</sup> R. J. Cava, B. Batlogg, K. Kiyono, H. Takagi, J. J. Krajewski, W. F. Peck Jr., L. W. Rupp Jr., and C. H. Chen, *Phys. Rev. B* **49**, 11890 (1994).
- <sup>5</sup> R. Greatrex, M. M. Greenwood, and M. Lala, *Mater. Res. Bull.* **15**, 113 (1980).
- <sup>6</sup> H. R. Oswald, S. Felder, E. Casagrande, and A. Reller, *Solid State Ionics* **63–65**, 565 (1993).
- <sup>7</sup> G. Xiao, M. Z. Cieplak, J. Q. Xiao and C. L. Chien, *Phys. Rev. B* **42**, R8752 (1990); K. Ishida, Y. Kitaoka, K. Yamazoe, K. Asayama, and Y. Yamada, *Phys. Rev. Lett* **76**, 531 (1996); M.-H. Julien, T. Feher, M. Horvatic, C. Berthier, O. N. Bakharev, P. Segransan, G. Collin, and J.-F. Marucco, *ibid* **84**, 3422 (2000).
- <sup>8</sup> M. Minakata and Y. Maeno, *Phys. Rev. B* **63**, 180504 (R) (2001).
- <sup>9</sup> K. Pucher, J. Hemberger, F. Mayr, V. Fritsch, A. Loidl, E.-W. Scheidt, S. Klimm, R. Horny, S. Horn, S. G. Ebbinghaus, A. Reller, and R. J. Cava, *Phys. Rev. B* **65**, 104523 (2002).
- <sup>10</sup> M. Braden, O. Friedt, Y. Sidis, P. Bourges, M. Minakata, and Y. Maeno, *Phys. Rev. Lett.* **88**, 197002 (2002).
- <sup>11</sup> N. Kikugawa and Y. Maeno, *Phys. Rev. Lett.* **89**, 117001 (2002).
- <sup>12</sup> K. Chandrasekaran, R. Vijayaraghavan, and U. V. Varadaraju, *Mater. Chem. Phys.* **56**, 63

- (1998).
- <sup>13</sup> T. Oguchi, Phys. Rev. B **51**, 1385 (1995).
- <sup>14</sup> W. Wong-Ng, H. McMurdie, B. Paretzkin, A. Kuchinski, and A. Dragoo, Powder Diff. **3**, 179 (1988).
- <sup>15</sup> C. N.R. Rao, D. D. Sarma, S. Vasudevan, and M. S. Hegde, Proc. Royal Soc. (London), Ser. A **367**, 239 (1979).
- <sup>16</sup> A. E. Bocquet, T. Mizokawa, K. Morikawa, A. Fujimori, S. R. Barman, K. Maiti, D. D. Sarma, Y. Tokura, and M. Onoda, Phys. Rev. B **53**, 1161 (1996).
- <sup>17</sup> S. Nakatsuji and Y. Maeno, Phys. Rev. B **62**, 6458 (2000).
- <sup>18</sup> T. Yokoya, A. Chainani, T. Takahashi, H. Katayama-Yoshida, M. Kasai, Y. Tokura, N. Shanthi, and D. D. Sarma, Phys. Rev. B **53**, 8151 (1996).
- <sup>19</sup> J. J. Yeh and I. Lindau, At. Data Nucl. Data Tables **32**, 1 (1985).
- <sup>20</sup> M. Pollak, Discuss. Faraday Soc. **50**, 7 (1970); V. Ambegaokar, B. I. Halperin, and J. S. Langer, Phys. Rev. B **4**, 2612 (1971); A. F. Efros and B. I. Shklovskii, J. Phys. C: Solid State Phys. **8**, L49 (1975); A. L. Efros, J. Phys. C: Solid State Phys. **9**, 2021 (1976); J. H. Davies, P. A. Lee, and T. M. Rice, Phys. Rev. B **29**, 4260 (1984); B. I. Shklovskii, and A. L. Efros, Sov. Phys.-Semicond. **14**, 487 (1980).
- <sup>21</sup> D. D. Sarma, S. R. Barman, H. Kajueter, and G. Kotliar, Europhys. Lett. **36**, 307 (1996); H. Kajueter, G. Kotliar, D. D. Sarma, and S. R. Barman, Int. J. Mod. Phys. B **11**, 3849 (1997); K. Maiti, Priya Mahadevan, and D. D. Sarma, Phys. Rev. Lett. **80**, 2885 (1998); D. D. Sarma, A. Chainani, S.R. Krishnakumar, E. Vescovo, C. Carbone, W. Eberhardt, O. Rader, Ch. Jung, Ch. Hellwig, W. Gudat, H. Srikanth, and A.K. Raychaudhuri, *ibid* **80**, 4004 (1998); K. Maiti, A. Kumar, D.D. Sarma, E.Weschke, and G. Kaindl, Phys. Rev. B **70**, 195112 (2004).

## FIGURE CAPTIONS

FIG. 1: (a) Ru  $3p$  spectral region with coincident Ti  $2p$  contribution from the  $\text{Sr}_2\text{Ru}_{1-x}\text{Ti}_x\text{O}_4$  series. (b) Ti  $2p$  spectra, extracted from the region shown in (a), from the same.

FIG. 2: Calculated density of states (DOS) from  $\text{Sr}_2\text{RuO}_4$  (a) and  $\text{Sr}_2\text{TiO}_4$  (b).

FIG. 3: XPS valence band spectra from the  $\text{Sr}_2\text{Ru}_{1-x}\text{Ti}_x\text{O}_4$  series at 300 K.

FIG. 4: He I narrow scan UPS spectra from the  $\text{Sr}_2\text{Ru}_{1-x}\text{Ti}_x\text{O}_4$  series at 300 K.

FIG. 5: BIS spectra from the  $\text{Sr}_2\text{Ru}_{1-x}\text{Ti}_x\text{O}_4$  series at 300 K.

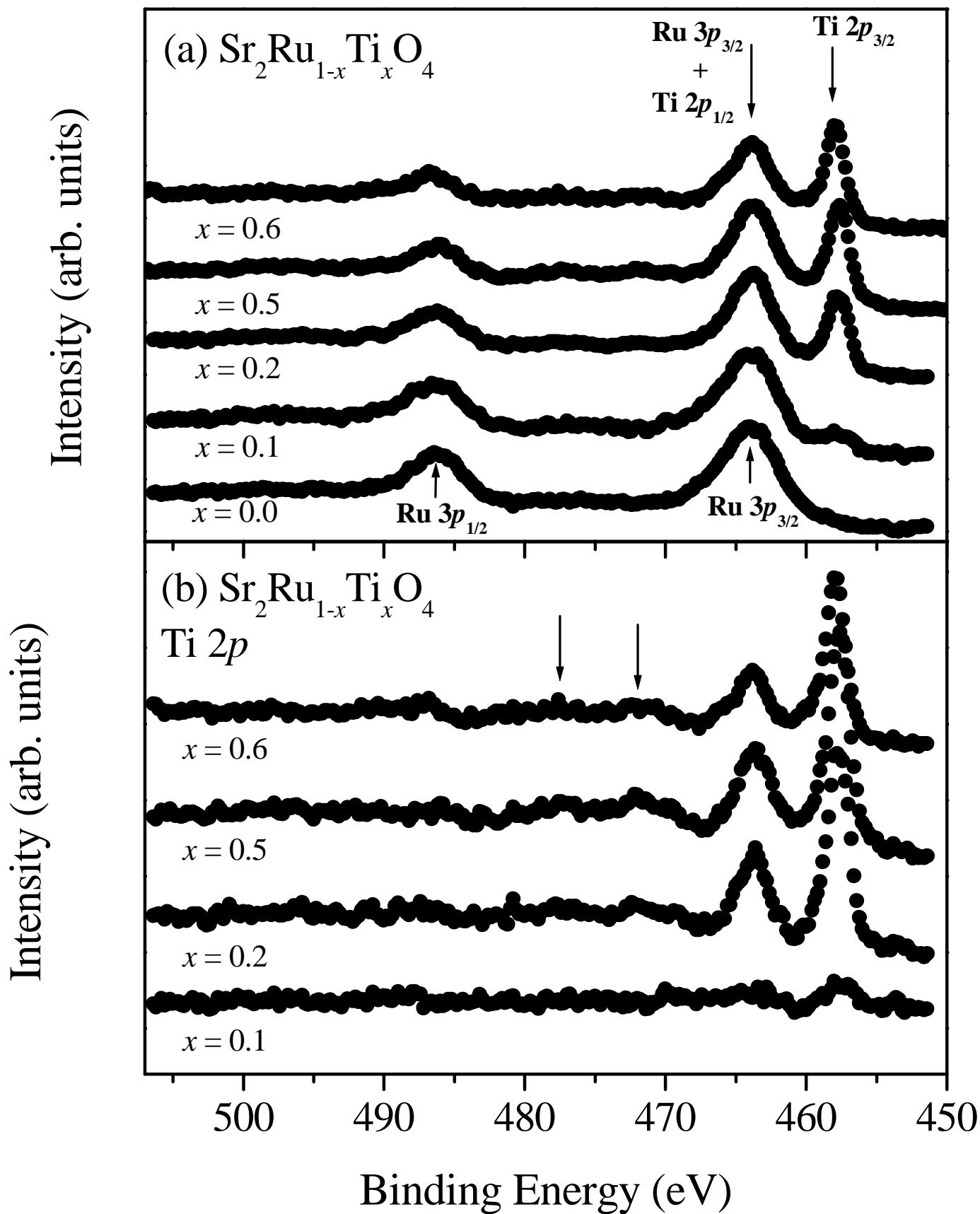


Fig. 1  
Ray *et al.*

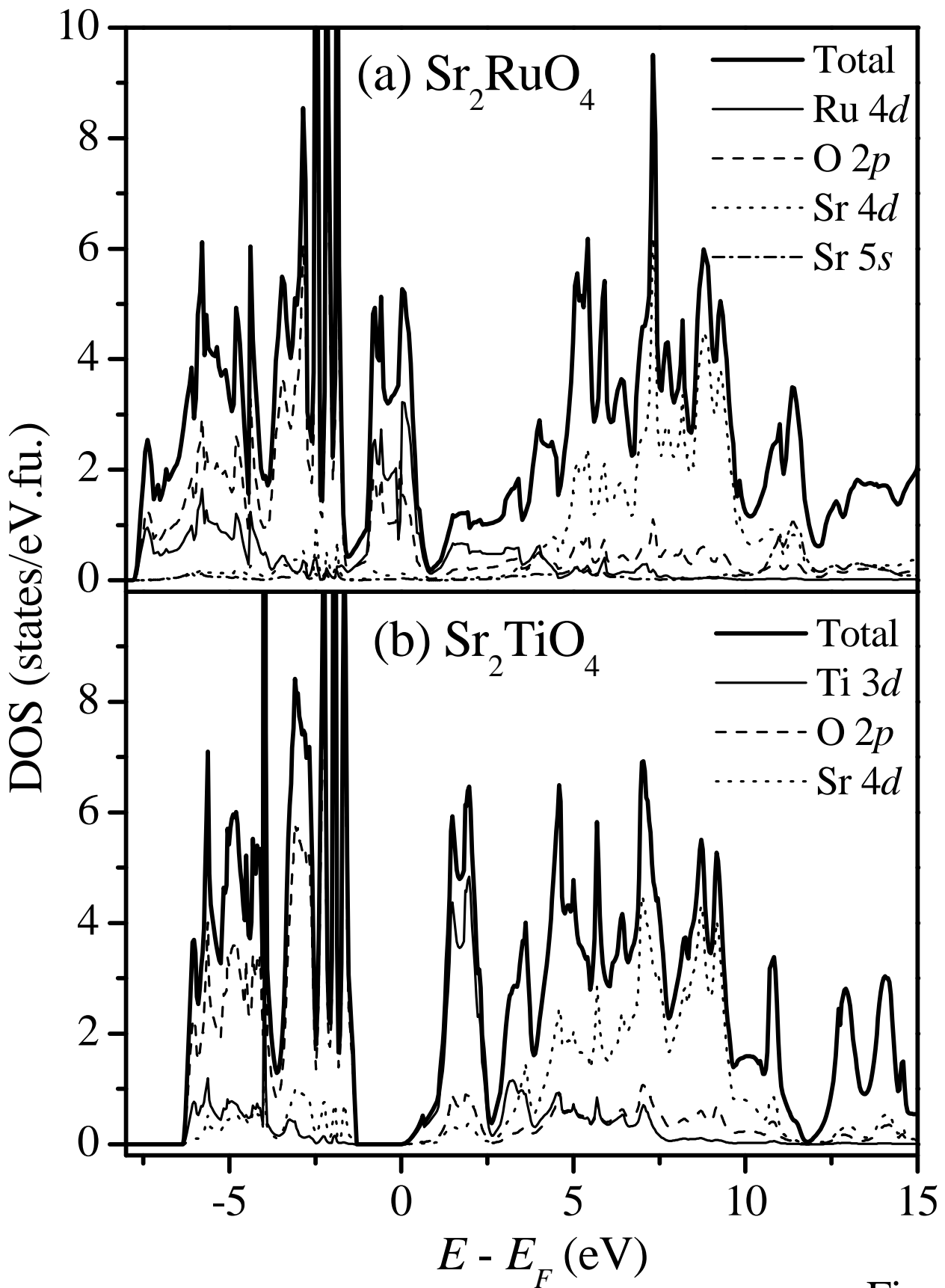


Fig. 2  
Ray *et al.*



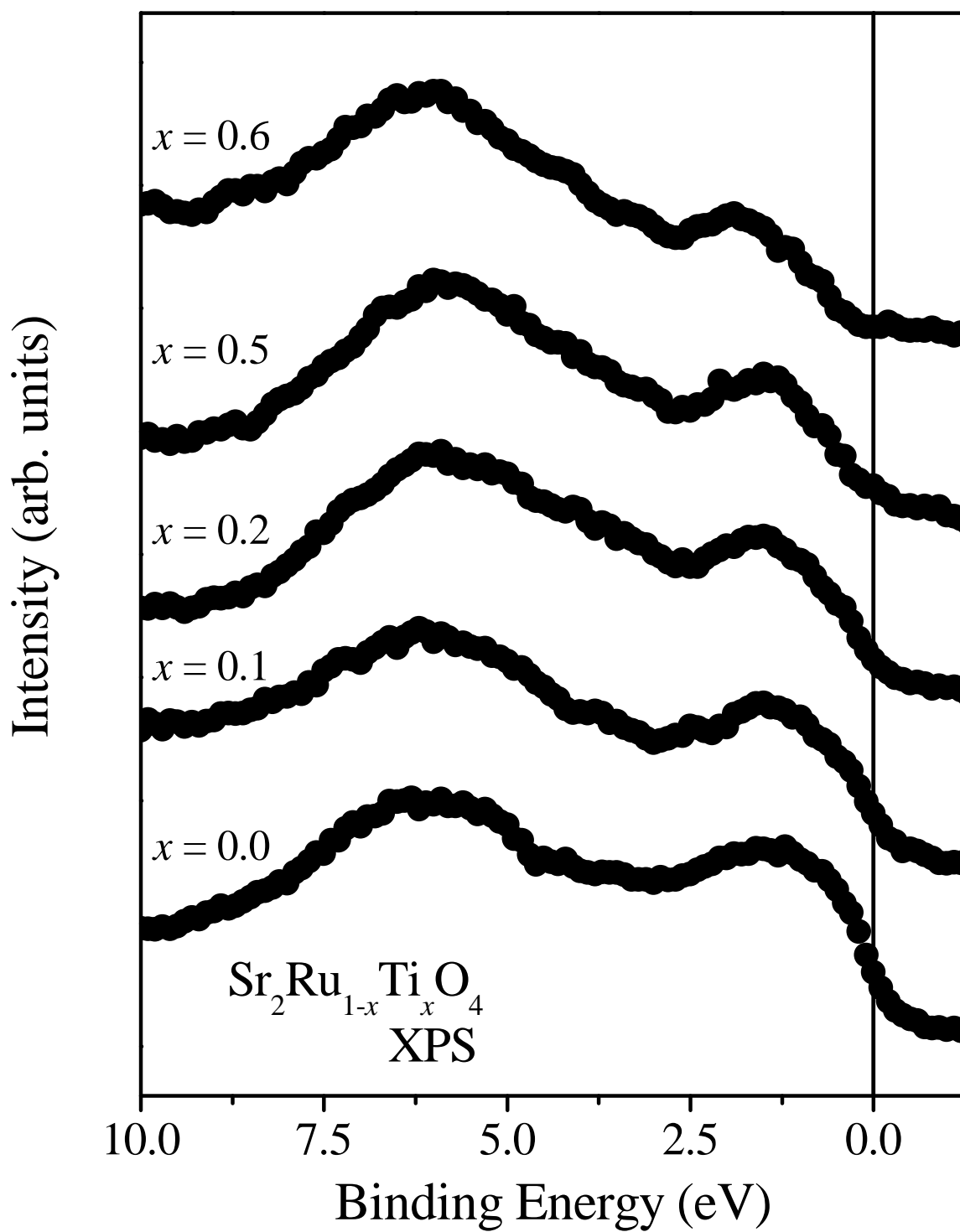


Fig. 3  
Ray *et al.*

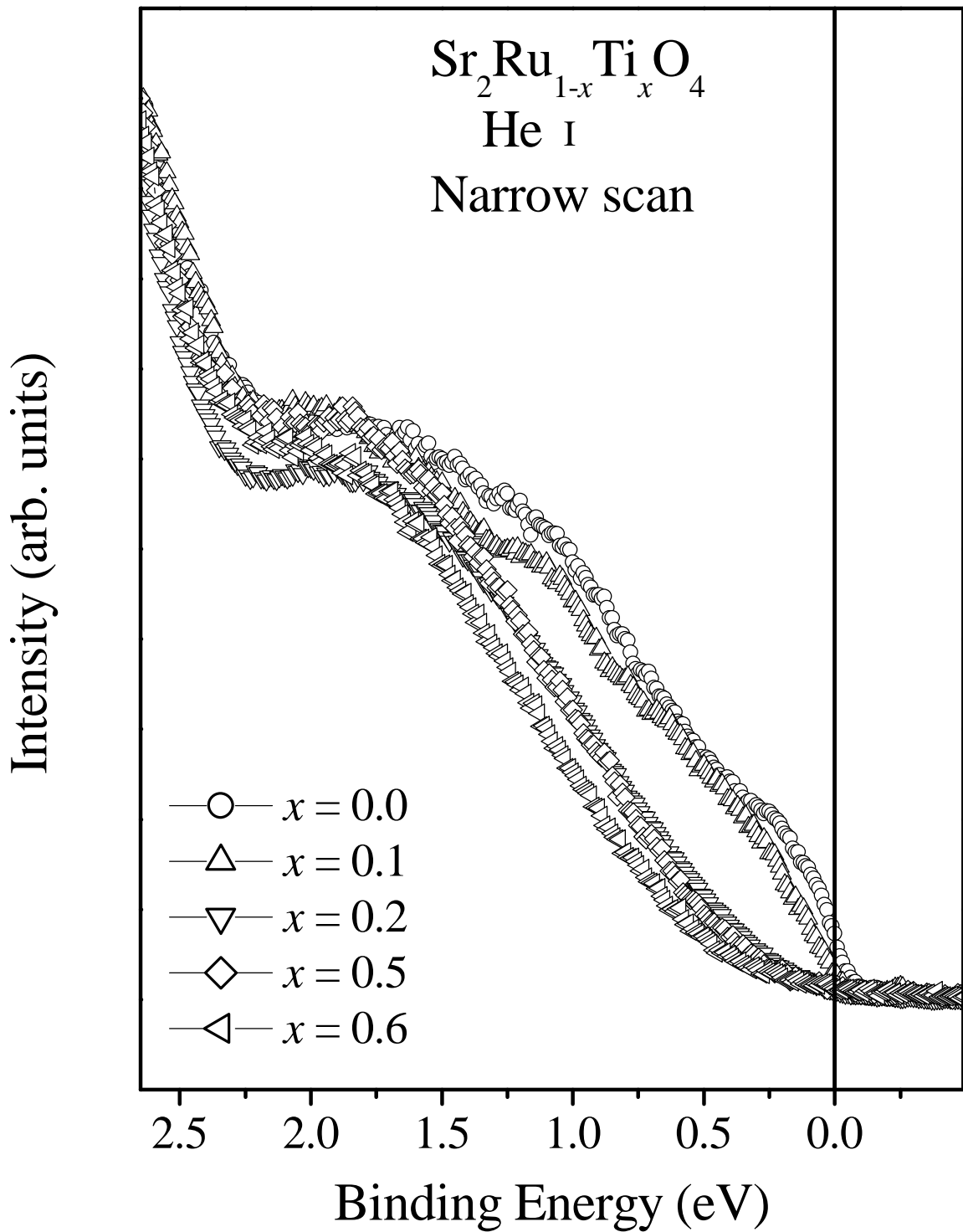


Fig. 4  
Ray *et al.*

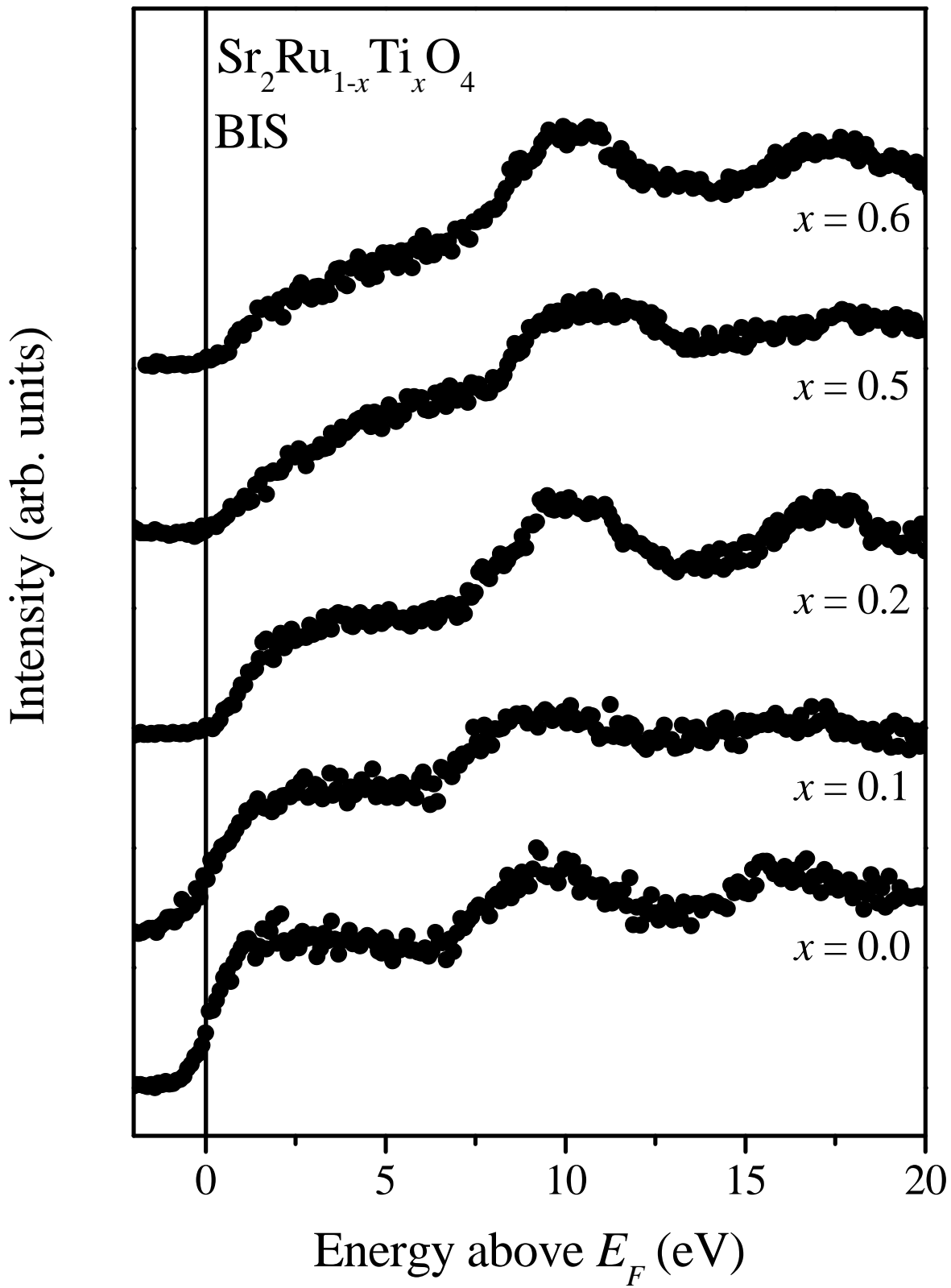


Fig. 5  
Ray *et al.*